Radiation quality correction factors for improved dosimetry in preclinical minibeam radiotherapy

Marios Sotiropoulos, Yolanda Prezado

Received: 24 December 2021 | Revised: 3 June 2022 | Accepted: 19 June 2022

DOI: 10.1002/mp.15838

RESEARCH ARTICLE

MEDICAL PHYSICS

Radiation quality correction factors for improved dosimetry in preclinical minibeam radiotherapy

Marios Sotiropoulos | **Yolanda Prezado**

Signalisation Radiobiologie et Cancer, CNRS UMR3347, Inserm U1021, Institut Curie, Université PSL, Orsay, France

Correspondence
Marios Sotiropoulos, Institut Curie Centre de Recherche, Campus Universitaire, Bâtiment 110, Orsay 91405, France.
Email: marios.sotiropoulos@curie.fr

Present address
Marios Sotiropoulos, Department of Radiation Oncology, Mayo Clinic, Rochester, MN, USA

Funding information
European Research Council (ERC), Grant/Award Number: 817908; Partnership for Advanced Computing in Europe (PRACE), Grant/Award Number: 2020225339

Abstract

Background: In reference dosimetry, radiation quality correction factors are used in order to account for changes in the detector's response among different radiation qualities, improving dosimetric accuracy.

Purpose: Reference dosimetry radiation quality corrections factors for the PTW microDiamond were calculated for preclinical X-ray and proton minibeams, and their impact in dosimetric accuracy was evaluated.

Methods: A formalism for the calculation of radiation quality correction factors for absolute dosimetry in minibeam fields was developed. Following our formalism, radiation quality correction factors were calculated for the PTW microDiamond detector, using the Monte Carlo method. Models of the detector, and X-ray and proton irradiation platform, were imported into the TOPAS Monte Carlo simulation toolkit. The radiation quality correction factors were calculated in the following scenarios: (i) reference dosimetry open field to minibeam center of the central peak, (ii) different positions at the minibeam profile (along the peaks and valleys direction) to the center of the central minibeam, and (iii) some representative depth positions. In addition, the radiation quality correction factors needed for the calculation of the peak-to-valley dose ratio at different depths were calculated.

Results: An important overestimation of the dose (about 10%) was found in the case of the open to minibeam field for both X-rays and proton beams, when the correction factors were used. Smaller differences were observed in the other cases.

Conclusions: The usage of the PTW microDiamond detector requires radiation quality correction factors in order to be used in minibeam reference dosimetry.

KEYWORDS
minibeams, microdiamond, Monte Carlo, radiation quality correction factors

1 | INTRODUCTION

Minibeam radiation therapy (MBRT) utilizes highly spatially fractionated dose distributions showing areas of high dose (peaks) and low dose (valleys).[1] This inhomogeneous dose distribution can achieve better normal tissue-sparing effect[2–8] and higher tumor control probability.[9–12] These promising results observed with minibeam radiotherapy have increased the research interest, with a large number of preclinical irradiations taken place. The improved efficacy of MBRT seems strongly related to the ratio between the peak and the valley dose at the entrance, the so-called peak-to-valley dose ratio (PVDR). As a result, the development of protocols for accurate routine dosimetry is necessary.

The dosimetry of minibeam dose distributions and quantification of the PVDR is challenging. Typical minibeam slit widths are between 0.2 and 1 mm

resulting to (partial) occlusion of the primary source in the beam axis and local charged particle equilibrium loss. Under these limitations, film dosimetry has been implemented in micro- and minibeam dosimetry[13–16] due to its two-dimensional nature, high spatial resolution, and weak energy dependence. Despite, typical film dosimetry requires many hours or even days after the irradiation to obtain the measurement results.[17]

Common detectors routinely used in small field dosimetry are still too large for the minibeams, whereas specialized detectors have not been commercially available. The small width of the minibeams requires detectors with active volume thickness in the order of a few micrometers. A potential candidate satisfying those requirements is a single-crystal diamond detector. These detectors have a thin layer of active volume, which can be placed perpendicular to the radiation field (edge-on orientation) providing a very high spatial resolution. The microDiamond (type 60019, PTW, Freiburg, Germany) solid-state dosimeter is a typical representative of this type of detectors. It has a 0.004 mm^3 cylindrical sensitive volume with a thickness of 1 μm and radius of 1.1 mm constituting it an ideal candidate for minibeam dosimetry. It has been extensively studied for use in photon, electron, and proton beam small fields[18–23] and has been used in micro- and minibeam measurements.[24,25]

The presence of the PTW microDiamond detector in a small field can introduce perturbations, and radiation quality correction factors might be necessary to correct for the perturbations and improve dosimetric accuracy, especially in the case of reference dosimetry. In synchrotron-based microbeam dosimetry, there is an indication that radiation quality correction factors for the PTW microDiamond might be needed.[24] Following this indication, Hugtenburg and Reynard[25] found that a correction factor of 1.144 ± 0.013 is needed for the evaluation of the PVDR with the microDiamond detector, demonstrating an important role of radiation quality correction factors in microbeam dosimetry.

In this work, we evaluated the improvements in the dosimetric accuracy when radiation quality correction factors are used in reference dosimetry for preclinical minibeam radiotherapy. For this purpose, we developed a formalism for the calculation of the radiation quality correction factors in minibeam radiotherapy. Then we applied the formalism in the calculation of radiation quality correction factors for the PTW microDiamond detector in typical preclinical X-ray and proton minibeam fields and demonstrated the impact of using the correction factors in the PVDR quantification. To the best of our knowledge, this is the first evaluation of this kind in the context of spatially fractionated radiation therapy and MBRT in particular.

2 | MATERIALS AND METHODS

2.1 | Minibeam radiation quality correction factors formalism

Typically, the clinical reference dosimetry is based on the measurement of the absorbed dose in water, D_w (e.g., TRS-398,[26] AAPM TG-51,[27] etc). The absorbed dose in water under reference conditions (denoted as "open"—see next paragraph) at depth d, $D_w^{open,d}$, is related to a measurement with the detector at depth d, $M^{open,\,d}$, through a calibration coefficient $N_{D,w}^{open,d}$:

$$D_w^{open,d} = M^{open,d} \cdot N_{D,w}^{open,d} \quad (1)$$

The irradiation setup in this case is the reference conditions described in the dosimetry protocol followed to obtain the calibration coefficient. This calibration is done in an open, broad beam, field (denoted as "open"), in contrast to a minibeam field, which is used in the following sections.

In the case of minibeams, the absorbed dose in water at the center of the central peak of a minibeam field at depth d (denoted as "$mini,x = 0,d$", see Figure 1) would be

$$D_w^{mini,x=0,d} = M^{mini,x=0,d} \cdot N_{D,w}^{open,d} \cdot k^{mini,x=0,d;open,d} \quad (2)$$

where the radiation quality correction factor, $k^{mini,x=0,d;open,d}$, was defined. The superscripts here denote the irradiation field and measurement details (i.e., detector position) that would normally affect the radiation quality. When a minibeam field is used, the exact position in the minibeam dose distribution has to be denoted. This is done by assuming a 2D Cartesian coordinates system, with the x-axis pointing toward the peaks and valleys. In addition, the depth of measurement (i.e., the z-axis) needs to be denoted. For example, "$mini,x = 0,y = 0,d = 1$ cm" would define the point in a minibeam distribution at $x = 0$ cm and $y = 0$ cm (i.e., the center of the distribution) at the depth of 1 cm. It can be easily inferred that when a parameter is not explicitly mentioned is considered 0, as in the case of an open field, where the measurement is done at the center of the field. When two field descriptors are required, they are separated by a semicolon. Here, we considered position at the center of the minibeam dose distribution ($y = 0$), and for simplicity, we do not explicitly denote the position at the y-axis. This radiation quality correction factor accounts for differences in field size, geometry, and beam quality between the open reference field used in the initial calibration of the detector and the

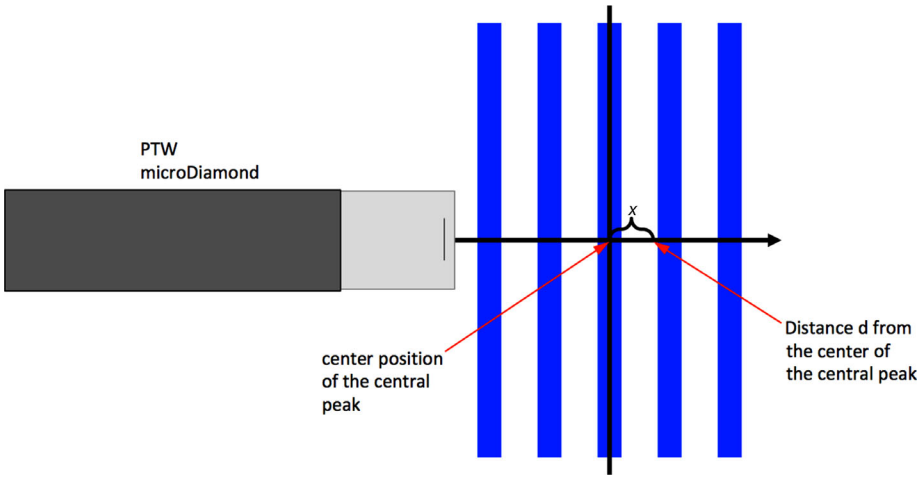

FIGURE 1 A minibeam field is shown with the peaks (blue) and valleys. The PTW microDiamond detector is placed at different positions along the direction of the peaks and valleys at a distance *x* from the center of the central peak.

minibeam field. It is given as follows:

$$k^{mini,x=0,d;open,d} = \frac{D_w^{mini,x=0,d}/M^{mini,x=0,d}}{D_w^{open,d}/M^{open,d}} \quad (3)$$

If the $k^{mini,x=0,d;open,d}$ radiation quality correction factors are available, the calibration coefficient of the open field can be used to calculate the absorbed dose in water at the center of the central peak of the minibeam field from a measurement with the detector at this point.

Instead of the center of the central peak, the correction factor can also be calculated for other positions in the minibeam distribution. However, it is more convenient to use the center of the central peak as an intermediate field/position. In this case, the absorbed dose in water at depth *d* and distance *x* from the center of the central peak along the peak and valley direction (denoted as "*mini,x,d*") is

$$\begin{aligned} D_w^{mini,x,d} &= M^{mini,x,d}\,.N_{D,w}^{mini,x=0,d}.k^{mini,x,d;mini,x=0,d} \\ &= M^{mini,x,d}\,.N_{D,w}^{open}.k^{mini,x,d;mini,x=0,d}.k^{mini,x=0,d;open,d} \end{aligned} \quad (4)$$

and the correction factor between the center of the central peak and distance *x* at depth *d* is defined as follows:

$$k^{mini,x,d;mini,x=0,d} = \frac{D_w^{mini,x,d}/M^{mini,x,d}}{D_w^{mini,x=0,d}/M^{mini,x=0,d}} \quad (5)$$

The calculation of a set of $k^{mini,x,d;mini,x=0,d}$ factors over the minibeam field will demonstrate the changes in the radiation quality between the center of the central peak and the rest of the minibeam dose distribution. If the difference is large, corrections might be necessary to improve dosimetric accuracy.

The radiation quality correction factors can be calculated implementing the Monte Carlo technique, using the following relation[28]:

$$k^{Q_1;Q_2} = \frac{D_w^{Q_1}/\bar{D}_{det}^{Q_1}}{D_w^{Q_2}/\bar{D}_{det}^{Q_2}} \quad (6)$$

where $D_w^{Q_1}$ and $D_w^{Q_2}$ is the absorbed dose in water, and $\bar{D}_{det}^{Q_1}$ and $\bar{D}_{det}^{Q_2}$ is the dose in the active volume of the detector, under irradiation conditions Q_1 and Q_2, respectively. Here it is noteworthy that the dose in water is calculated to a point, whereas the dose in the detector is calculated in the active volume (and material) of the detector.[28]

The two methods for calculating the correction factor are related as follows:

$$\begin{aligned} k^{Q_1;Q_2} &= \frac{D_w^{Q_1}/\bar{D}_{det}^{Q_1}}{D_w^{Q_2}/\bar{D}_{det}^{Q_2}} = \frac{D_w^{Q_1}/(M^{Q_1}.W_{det}^{Q_1})}{D_w^{Q_2}/(M^{Q_2}.W_{det}^{Q_1})} \\ &= \frac{D_w^{Q_1}/M^{Q_1}}{D_w^{Q_2}/M^{Q_2}}.\frac{W_{det}^{Q_2}}{W_{det}^{Q_1}} \end{aligned} \quad (7)$$

where $W_{det}^{Q_1}$ and $W_{det}^{Q_2}$ is the average energy to create an electron–hole (or electron–ion) pair. Typically, the *W* values have a small dependence to the beam quality and the ratio $W_{det}^{Q_2}/W_{det}^{Q_1}$ can be considered constant and equal to unity when similar radiation qualities are used.

2.2 | Simulation geometry

For all simulations, the TOPAS v3.2 simulation software was used.[29,30] Within this environment, models of the

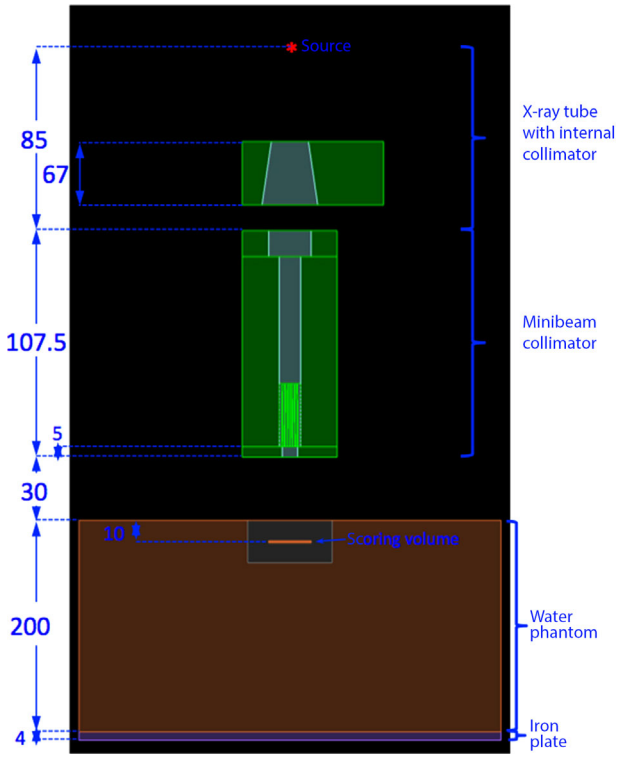

FIGURE 2 Simulation geometry at the small animal radiotherapy research platform (SARRP) in the minibeam setup. All dimensions are in mm.

detector, and the X-ray and proton irradiation platforms, were built.

2.2.1 | X-ray source

A simple geometry of the X-ray tube of the small animal radiotherapy research platform (SARRP—Xstrahl Inc., Swanee, GA, USA) was created for the simulations (Figure 2). The geometry consists of an X-ray source and the internal brass collimator of the tube. When the minibeam collimator was needed, it was placed at the front of the internal collimator. The photons of the source were initiated from the focal plane of the X-ray tube. Their spatial distribution was sampled from a Gaussian with a sigma of 0.75 and 0.25 mm for the *x*- and *y*-direction and a cutoff value of 3 and 1 mm, respectively. The angular distributions were uniform in both directions, with an angle of 20°. The spectrum was generated using the SpekPy software toolkit.[31,32] The tube parameters at treatment mode were selected. At this mode, the large spot is used at 220 kV tube potential. The tube has an inherent 0.8 mm beryllium filter, with an additional 0.15 mm copper filter in the treatment mode. The permanent ionization chamber installed in our system adds another 0.1 mm copper-equivalent filtration. For more details in the validation of the X-ray tube model, see Section S1.

For the minibeam generation, the previously developed preclinical collimator[6] was modeled and included in the simulation. In contrast to the previous work, the position of the collimator is now 1.275 mm downstream, due to the addition of the ionization chamber. In short, the brass collimator has seven divergent slits of about 400 μm width and 20 mm length at a center-to-center distance of 1.6 mm. For use in small animal irradiations, the minibeam field is further reduced by a 5 mm thick, 7 mm $\times$ 7 mm square brass collimator at the exit of the minibeam collimator, which results in having five different minibeams.

For simulation efficiency, the particle split variance reduction method was used. In this method, when a photon was reaching the phantom surface, it was duplicated 10 times with a weight of 1/10 = 0.1.

In all the X-ray simulations, the "g4em-standard_opt3" physics list was used with a cutoff value for all particles of 0.005 mm.

2.2.2 | Proton beamline

For the proton irradiation, the ICPO proton therapy beamline was assumed (Figure 3). The model and the parameterization of the ICPO pencil beam scanning nozzle previously reported were used.[33,34] In this model, the beam at the vacuum window is defined by its parameters at the isocenter. The simulation transports the proton beam from the vacuum window to the isocenter and includes the scanning magnets and both ionization chamber monitors.

The 6.5 cm thick brass collimator is placed at the nozzle exit. It has five divergent slits of 400 μm width and 20 mm length at a center-to-center distance of 2.8 mm, as this is a typical setup we use for preclinical irradiations.

In TOPAS, a typical modular physics list for proton therapy was used.[33,34] The cutoff value for all particles is 0.05 mm. In order to increase efficiency, the particle split variance reduction method was used. Two particle split planes were placed, one after the ionization chamber number 2 (in Figure 3) and one after the collimator; the particle split number was 10 for each split plane.

2.2.3 | The PTW microDiamond

The TOPAS model of the PTW microDiamond detector (type 60019) was created based on the technical drawing provided from PTW that provided dimensions and material composition of the detector internal structure. In the simulation, the active volume is a cylindrical volume of 1 μm thickness and 1.1 mm radius consisting of carbon with a density of 3.53 g/cm^3.

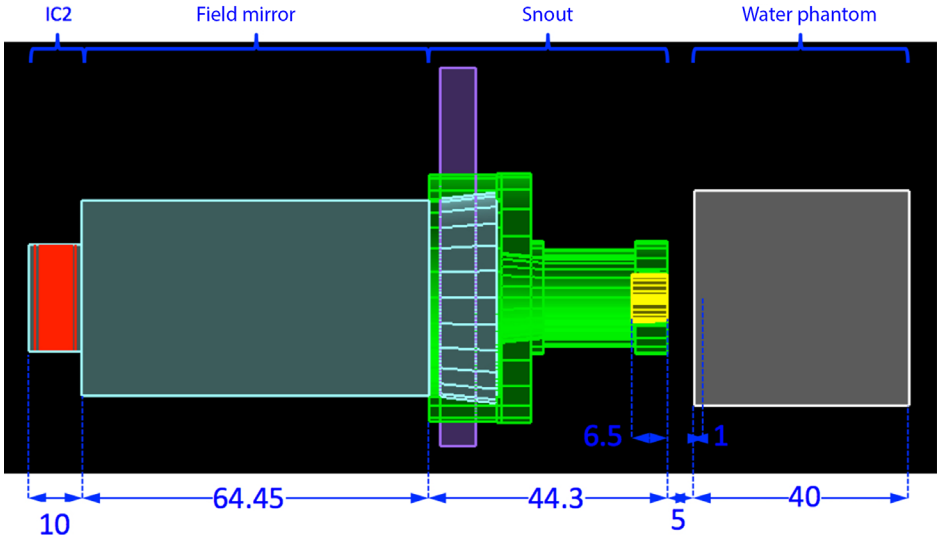

FIGURE 3 ICPO proton therapy beam line exit section, from the second ionization chamber to the collimator exit. All dimensions are in cm.

2.3 | Calculations using the Monte Carlo method

2.3.1 | Radiation quality correction factors

The PTW microDiamond detector was placed perpendicular to the radiation field on the direction of the peaks and valleys of the minibeam distribution (see Figure 1). The same orientation for the detector was used with the open field irradiations. The calculations were made at typical minibeam fields routinely used in preclinical experiments at our lab.

The simulations provided values for the D_w and $\bar{D}_{det}$ for the open fields and minibeam fields in order to calculate the $k^{mini,0,d;open,d}$ radiation quality correction factor between the reference calibration open field and the center of the central minibeam, and the $k^{mini,x,d;mini,x=0,d}$ correction factor between the center of the central minibeam and the minibeam position at distance x.

As the radiation quality can change significantly with depth, the radiation quality correction factors were also calculated at different depths relative to the reference depth. Some representative depths were selected for this purpose, and only the central peak ($x = 0$) and first valley correction factors were calculated.

2.3.2 | Corrected peak-to-valley dose ratio values

The PVDR is a common quality index in minibeam dose distributions. To demonstrate the improvement when using the radiation quality correction factors, a comparison between corrected and uncorrected PVDR was performed. The corrected PVDR between the central peak and the first valley was calculated as

$$PVD\ R^{d}_{corr} = \frac{D_w^{mini,x=0,d}}{D_w^{mini,x=valley,d}} = \frac{\bar{D}_{det}^{mini,x=0,d}}{\bar{D}_{det}^{mini,x=valley,d}} \cdot \frac{1}{k^{mini,x=valley,d;mini,x=0,d}} \quad (8)$$

which shows that the corrected PVDR is inversely proportional to the radiation quality correction factor at the valley.

2.3.3 | PTW microDiamond directional dependence

Assuming that the microDiamond detector is not symmetrical, different rotations were simulated in order to evaluate the asymmetry of the design. The effect might come from the asymmetrical internal structure (electrodes and supporting structure) that includes some structures with high atomic number materials. Two cases were evaluated: (i) a 90° rotation along the main axis and (ii) a 180° rotation in an axis perpendicular to the main axis and through the active volume.

3 | RESULTS

Using the formalism developed, reference dosimetry radiation quality correction factors were calculated for the PTW microDiamond detector. The radiation quality correction factors were calculated in the case of (i) the reference calibration open field and the center of the central minibeam peak and (ii) the central minibeam peak and other positions in the minibeam profile, that

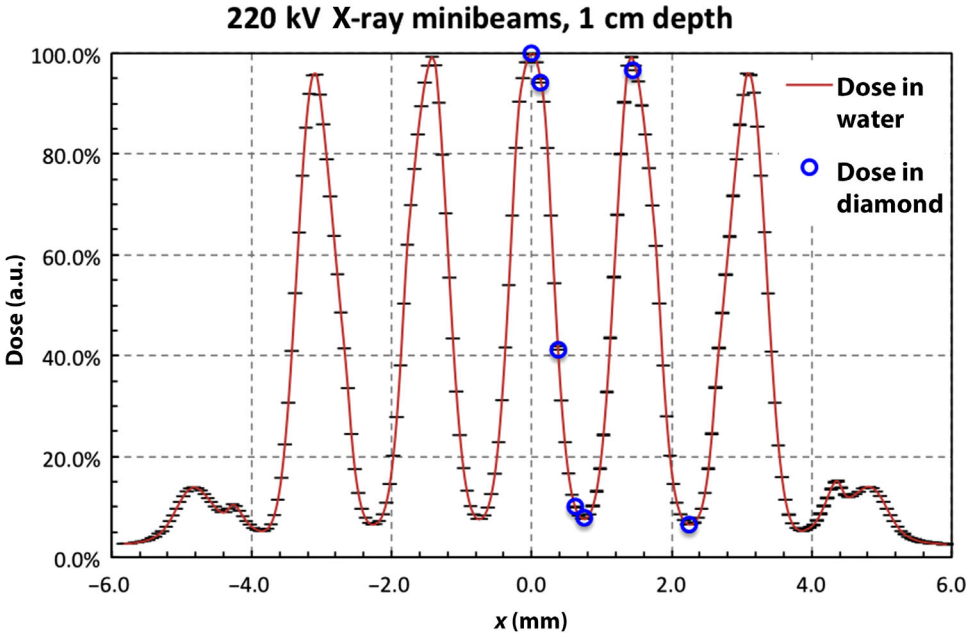

FIGURE 4 Minibeam percentage profiles calculated in water and in diamond material for the 220 kV X-ray minibeams at 1 cm depth

TABLE 1 Radiation quality correction factors for the 220 kV X-ray minibeams, from the reference open field to central minibeam peak

SSD (cm)	Minibeam depth @ 1 cm	
	$k^{\min i,x=0,d=1\text{cm};open,d}$	$\sigma_{k^{\min i,0;open}}$
19.45	0.944	0.002
33.00	0.925	0.006

Note: The open field is at the minibeam (SSD = 19.45 cm, detector depth = 1 cm) or reference conditions (SSD = 33.00 cm, detector depth = 2 cm) setup.

is, positions in the peaks, valleys, and, in between, at different depths. Using the calculated radiation quality correction factors, PVDR values were evaluated in order to estimate the impact of the correction factors to the PVDR.

3.1 | X-ray minibeam radiation quality correction factors

Radiation quality correction factors between the open field at the reference setup (open field about 10 × 10 cm^2, SSD = 33.00 cm, depth = 2 cm) or the minibeam setup (open field about 10 × 10 cm^2, SSD = 19.45 cm, depth = 1 cm) and the center of the central minibeam peak for the 220-kV X-rays (minibeam collimator, SSD = 19.45 cm, depth = 1 cm) are presented in Table 1. These correction factors show an important change (~6%–8%) between the open field and the center of the central peak of the minibeam distribution, indicating the need for correction factors when the microDiamond detector has been calibrated in an open field.

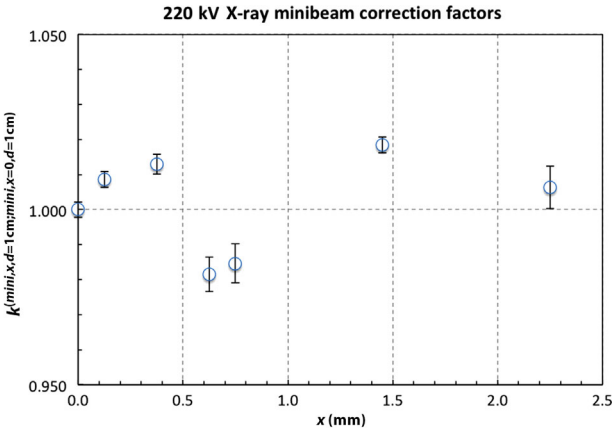

FIGURE 5 Radiation quality correction factors for the 220 kV X-ray minibeams between the central minibeam peak and off-axis positions at the minibeam profile, at 1 cm depth

Figure 4 shows the minibeam percentage profiles calculated in water and in diamond at 1 cm depth for the 220 kV X-ray minibeams. The position where the dose in diamond is calculated is the position where the radiation quality correction factors are calculated. The correction factors between the center of the central minibeam and at distance x are shown in Figure 5. A difference of ±1.8% is observed for the off-axis correction factors demonstrating only a small radiation quality change between peaks and valleys. At greater depths (Figure 6, see also Figures S5 and S6 for the depth–dose profile and profiles at different depths), there is a small change in the radiation quality correction factors, less than 3%, demonstrating again a small dependence of the correction factor with the depth.

TABLE 2 Radiation quality correction factors for 100 and 160 MeV proton minibeams, from the open field to central minibeam peak

Field size (cm^2)	Open field depth (cm)	100-MeV protons		160-MeV protons	
		$k^{min\ i,x=0,d;open,d}$	$\sigma_{k^{min\ i,x=0,d;open,d}}$	$k^{min\ i,x=0,d;open,d}$	$\sigma_{k^{min\ i,x=0;open,d}}$
	Minibeam depth @ 1 cm				
4 × 4	1	0.904	0.007	N/A	
	2	0.897	0.014	N/A	
10 × 10	1	0.912	0.019	0.891	0.014
	2	0.884	0.007	0.884	0.012
	Minibeam depth @ 2 cm				
4 × 4	1	0.910	0.007	N/A	
	2	0.903	0.014	N/A	
10 × 10	1	0.918	0.019	0.897	0.014
	2	0.890	0.007	0.890	0.012

Note: The correction factor is calculated in two different open field sizes and two minibeam depths.

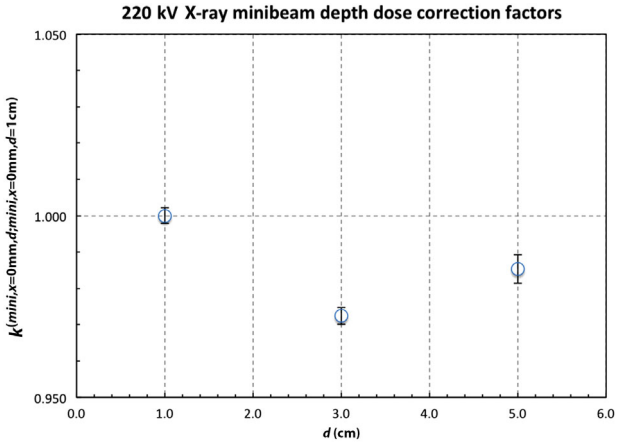

FIGURE 6 Radiation quality correction factors for the central minibeam peak at different depths with respect to the 1 cm depth for the 220 kV X-ray minibeams

3.2 | Proton minibeam radiation quality correction factors

Table 2 shows the radiation quality correction factors between the open field and the center of the central peak for the 100 and 160 MeV protons. The open field is either 4 × 4 or 10 × 10 cm^2 and the measurement depth for the open field is either 1 or 2 cm. The minibeams are measured at a depth of 1 or 2 cm. Again, an important correction of about 10% is required when the PTW microDiamond calibration is given in an open field but is intended to be used in a minibeam field.

Figures 7 and 8 show the percentage minibeam profiles at 1 and 2 cm and the dose in the PTW microDiamond for the 100- and 160-MeV proton minibeams, respectively. The corresponding minibeam radiation quality correction factors are shown in Figures 9 and 10. The correction factor significantly increases from the peak to the valley, exhibiting a difference of around 10%

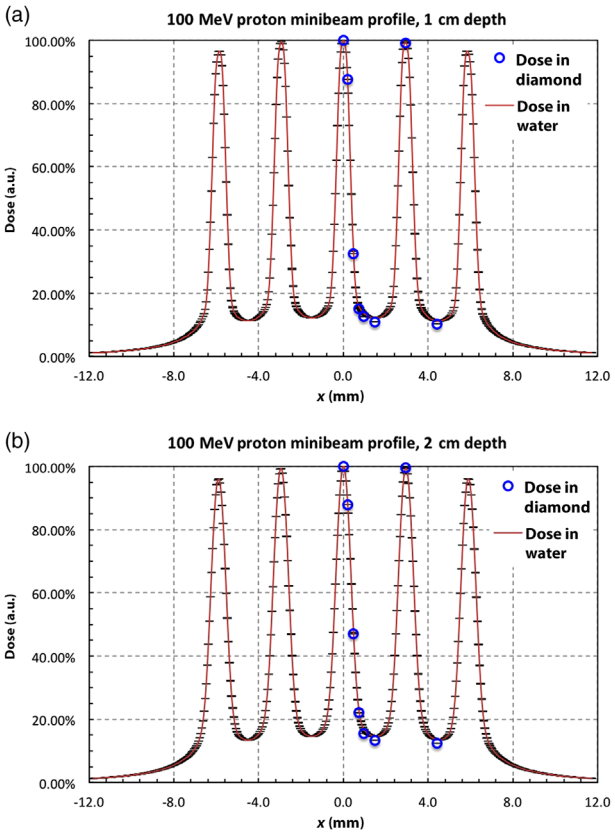

FIGURE 7 Minibeam percentage profiles calculated in water and in diamond material for the 100 MeV proton minibeams at (a) 1 and (b) 2 cm depth

in the valleys. This demonstrates a significant change in the radiation quality in the valleys, which leads to change in the detector response. The correction factors for the depth–dose profiles (see Figures S7–S9 in for the percentage depth–dose profiles and minibeam profiles) are presented in Figures 11 and 12, respectively. Differences with the depth are of the order of 2% and 5% for the 100 and 160 MeV proton minibeams.

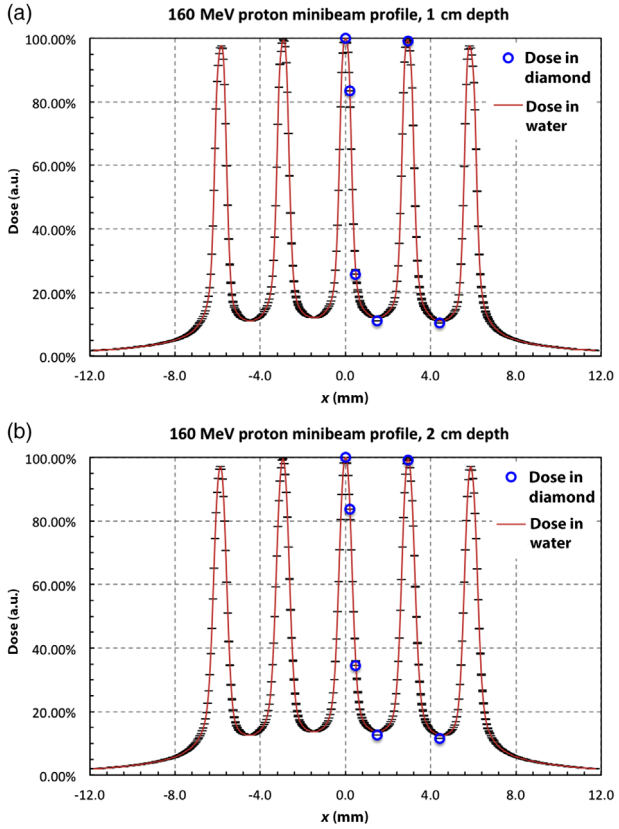

FIGURE 8 Minibeam percentage profiles calculated in water and in diamond material for the 160 MeV proton minibeams at (a) 1 and (b) 2 cm depth

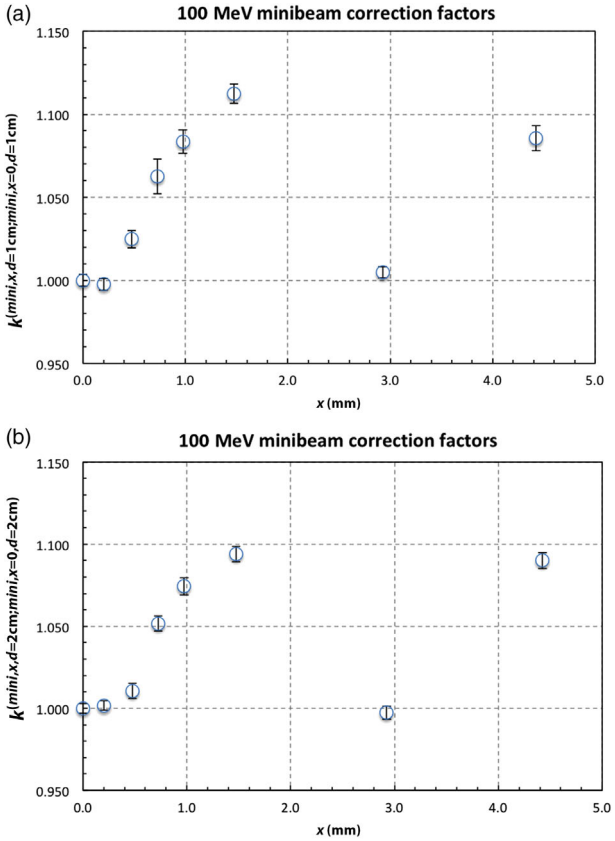

FIGURE 9 Radiation quality correction factors for the 100 MeV proton minibeams between the central minibeam peak and off-axis positions at the minibeam profile at (a) 1 and (b) 2 cm depth

Here, it is worthy to mention that depth–dose profiles at the center of a minibeam exhibit steep gradients (see Figure S7), and some dose averaging effects might be present.

3.3 | Uncertainty in the peak-to-valley dose ratio

A common index in the minibeams treatments is the PVDR. In this section, the PVDR of the main peak and the valley next to it is calculated. Table 3 shows the corrected (i.e., using the radiation quality correction factor) and uncorrected (i.e., without using the radiation quality correction factor) PVDR data for the radiation qualities studied. Although the correction in the X-rays is small, the corrections for the protons are quite important for most depths. The difference is around 10% for the low-energy protons. In the higher energy protons, the correction varies between about 3% and 9%, excluding the cases where the peaks and valley dose distribution is not observed and has been merged (i.e., depths of 12 and 16 cm, see depth–dose profile in Figure S7). In protons, there is a decrease in the difference between the corrected and uncorrected PVDR with depth; shallow depths have greater PVDR differences.

3.4 | PTW MicroDiamond directional dependence

The directional dependence of the PTW microDiamond detector is shown in Table 4. Overall, the difference in dose measured with a rotated detector is less than 0.65%, demonstrating a negligible dependence on the orientation. This result is in-line with previous findings in photon small field dosimetry.[23]

4 | DISCUSSION

In this work, we evaluated the improvements in the dosimetric accuracy in minibeam preclinical radiotherapy when radiation quality correction factors are used in reference dosimetry. For this purpose, a formalism for the calculation of the radiation quality correction factors was developed and applied in typical scenarios. In the proposed formalism, the absorbed dose in water at a minibeam profile is divided into two steps: (i) The dose at the center of the central beam is calculated, and (ii) the dose at the minibeam profile is calculated. This two-step approach generates the need for two types of correction factors: (i) between the open field where the detector has

TABLE 3 Peak-to-valley dose ratio (PVDR) calculated with (corrected) and without (uncorrected) the radiation quality correction factors for the radiation qualities studied

Radiation type	Depth (cm)	$k_{mini,x=valley,d;\ mini,x=0,d}$	σ_k	$PVDR_{uncorr}$	$\sigma_{PVDRuncorr}$	$PVDR_{corr}$	$\sigma_{PVDRcorr}$	Difference (%)
X-rays								
220 kV	1	0.985	0.006	12.85	0.06	13.05	0.09	−1.5
	3	0.995	0.007	6.34	0.03	6.37	0.05	−0.5
	5	0.960	0.008	3.90	0.02	4.06	0.04	−4.0
Protons								
100 MeV	1	1.112	0.006	9.10	0.04	8.18	0.06	11.2
	2	1.094	0.005	7.47	0.03	6.83	0.04	9.4
	4	1.109	0.005	3.58	0.01	3.22	0.02	10.9
	6	1.119	0.003	1.46	0.00	1.30	0.01	11.9
160 MeV	1	1.090	0.010	8.99	0.07	8.25	0.10	9.0
	2	1.084	0.008	7.90	0.05	7.29	0.07	8.4
	4	1.068	0.008	5.17	0.04	4.84	0.05	6.8
	8	1.031	0.019	1.41	0.03	1.37	0.04	3.1
	12	0.999	0.006	1.01	0.01	1.01	0.01	−0.1
	16	0.995	0.005	1.01	0.00	1.01	0.01	−0.5

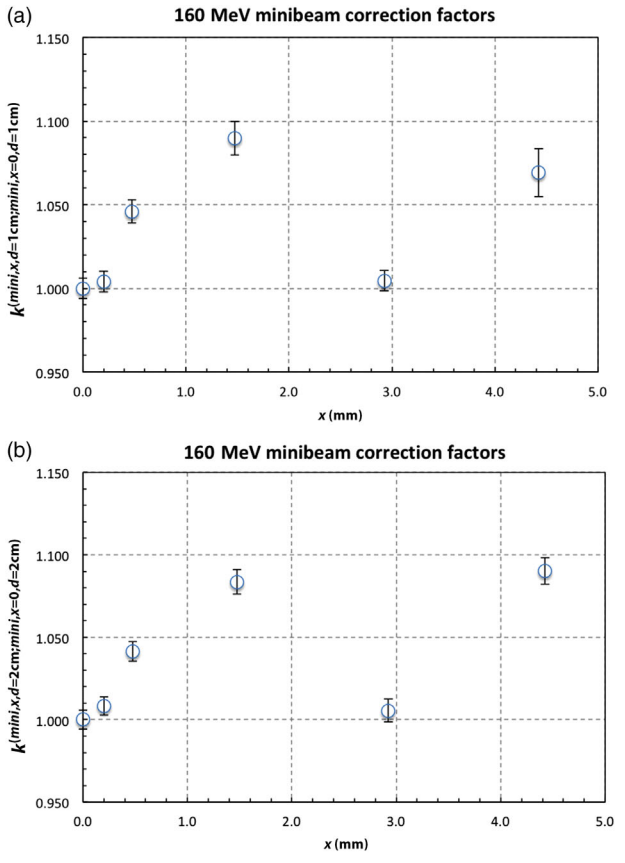

FIGURE 10 Radiation quality correction factors for the 160 MeV proton minibeams between the central minibeam peak and off-axis positions at the minibeam profile at (a) 1 and (b) 2 cm depth

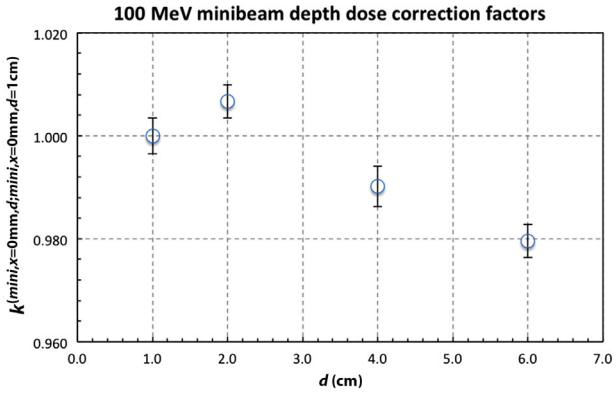

FIGURE 11 Depth–dose radiation quality correction factors for the central minibeam peak at different depths with respect to the 1 cm depth for the 100 MeV proton minibeams

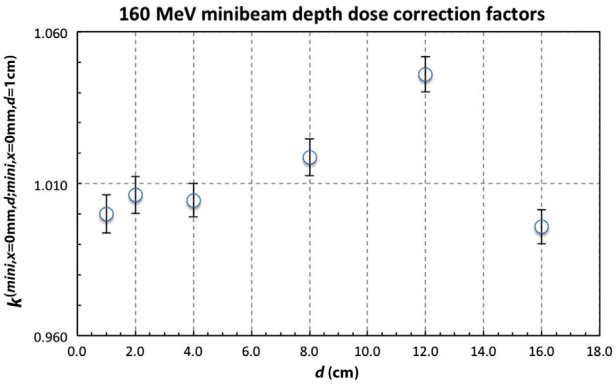

FIGURE 12 Depth–dose radiation quality correction factors for the central minibeam peak at different depths with respect to the 1 cm depth for the 160 MeV proton minibeams

TABLE 4 Difference between the rotated and un-rotated PTW microDiamond detectors

Rotation (°)	Radiation quality	Depth (cm)	Difference (%)
θ			
90	X-rays	1	0.17
90	100-MeV protons	1	−0.15
90	100-MeV protons	2	−0.16
φ			
180	X-rays	1	0.25
180	100-MeV protons	1	0.64
180	100-MeV protons	2	0.17

Note: With theta, θ, is a rotation around the main axis and with phi, φ, is a rotation perpendicular to the main axis through the active volume.

been calibrated and the center of the central peak in the minibeam profile, and (ii) between the center of the central peak in the minibeam profile and at distance x from it. Following the proposed formalism, the impact of the correction factors in the dosimetric accuracy was evaluated for the PTW microDiamond detector for orthovoltage X-rays (220 kV) and proton (100 and 160 MeV) minibeam fields.

The correction factors for the PTW microDiamond detector between the open field and the central peak in the minibeam profile, $k^{\min i,x=0,d;open,d}$, are important in both (X-rays and protons) radiation qualities. For the typical reference dosimetry setup for 220 kV X-rays at our lab (field size is about 10 × 10 cm^2, which is achieved without a collimator, SSD = 33 cm, depth = 2 cm) and a minibeam profile at 1 cm depth (SSD = 19.45 cm), the correction is 8%. In protons (reference setup: 10 × 10-cm^2 field, 2 cm depth; minibeams at 1 cm depth) the correction is around 10%. That is expected as the radiation quality, and therefore the detector response is expected to significantly change between the open field and the central minibeam. These results demonstrate the need to generate quality correction factors when radiation detectors are used for determination of the absorbed dose in water at a minibeam array, especially at shallow depths.

The correction factors for the microdiamond detector between the central peak in the minibeam profile and distance x along the peak and valley direction, $k^{\min i,x,d;\min i,x=0,d}$, are important in the case of protons. For X-ray minibeams, the correction is around 1.5% and is close to the measurement uncertainty so in a first approximation could be neglected. In proton minibeams, the dose at the valleys is underestimated, and a correction of around 10% is required. This large difference is expected due to the change in the spectrum and LET_d in the valleys in comparison to the peaks[35] that affect the detector response.

The significance of the profile corrections factors, $k^{\min i,x,d;\min i,x=0,d}$, is demonstrated in PVDR calculations. PVDR is very sensitive to changes in peak or valley dose. In our formalism, PVDR is directly proportional to the $k^{\min i,x=valley,d;\min i,x=0,d}$ correction. Consequently, PVDR differences between uncorrected and corrected are −1.5% for the X-ray minibeams and get more important in proton minibeams, around 10%.

Due to the physical dimensions of the PTW microDiamond detector minibeam profiles only along the peak and valley direction are possible. Indeed the diameter of the microDiamond is 2.2 mm and when compared with the length of the minibeams studied (~2 cm) can expect strong averaging effects, especially near the edge of the field.

Getting accurate measurements of the minibeam profiles and in particular the peak and valley dose and the PVDR is crucial for quantifying the MBRT effect.[36] This work highlights the need for using minibeam field–specific radiation quality correction factors with measurements with the PTW microDiamond detector in the reference dosimetry of minibeams. We hope that this work would be a guide for other groups to conduct their own measurements and calculations in order to generate radiation quality correction factors valid and specific for their conditions.

At the same time, we can note the limitations in creating a dosimetry protocol for minibeams: At the moment, there is not a standard for describing the minibeam field, and there is not a minibeam radiation quality index. More importantly, due to the sharp gradient typically found in minibeam dose distributions, lot of attention needs to be taken during a measurement. Defining a position in a minibeam profile might be complicated, and only the peaks and the valleys might be possible to define with enough precision. In this study, by using Monte Carlo simulations, we were able to demonstrate the situation in an idealized environment in order to initiate the discussion for accurate reference dosimetry in MBRT. We expect that this discussion would become more important toward the clinical implementation of MBRT.

5 | CONCLUSIONS

Radiation quality correction factors were calculated for reference dosimetry with the PTW microDiamond detector in a series of X-ray and proton minibeam fields typically used in small animal irradiations. Our calculations demonstrated that a notable correction factor is involved when the detector is calibrated in an open field but is intended to be used in a photon or proton minibeam field. In addition, an important effect of the correction factors to the PVDR was shown for proton minibeam, whereas for the X-rays, the correction was small. Overall, the inclusion of radiation quality correction factors in minibeam dosimetry with the PTW

microDiamond detector results in differences in the dose of around 5% and 10% for photons and proton minibeams, respectively.

ACKNOWLEDGMENTS

This project has received funding from the European Research Council (ERC) under the European Union's Horizon 2020 research and innovation programme (Grant no. 817908). We acknowledge PRACE for awarding us access to computational cluster Joliot Curie-SKL (France) under Grant no. 2020225339.

CONFLICT OF INTEREST

The authors do not have any relevant conflicts of interest to disclose.

REFERENCES

1. Meyer J, Eley J, Schmid TE, Combs SE, Dendale R, Prezado Y. Spatially fractionated proton minibeams. *Br J Radiol*. 2019;92(1095):20180466. https://doi.org/10.1259/bjr.20180466
2. Dilmanian FA, Zhong Z, Bacarian T, et al. Interlaced x-ray microplanar beams: a radiosurgery. *Natl Acad Sci USA*. 2006;103(25):9709-9714.
3. Deman P, Vautrin M, Edouard M, et al. Monochromatic minibeams radiotherapy: from healthy tissue-sparing effect studies toward first experimental glioma bearing rats therapy. *Int J Radiat Oncol*. 2012;82(4):e693-e700. https://doi.org/10.1016/j.ijrobp.2011.09.013
4. Prezado Y, Deman P, Varlet P, et al. Tolerance to dose escalation in minibeam radiation therapy applied to normal rat brain: long-term clinical, radiological and histopathological analysis. *Radiat Res*. 2015;184(3):314-321. https://doi.org/10.1667/rr14018.1
5. Girst S, Greubel C, Reindl J, et al. Proton minibeam radiation therapy reduces side effects in an in vivo mouse ear model. *Int J Radiat Oncol*. 2016;95(1):234-241. https://doi.org/10.1016/j.ijrobp.2015.10.020
6. Prezado Y, Dos Santos M, Gonzalez W, et al. Transfer of minibeam radiation therapy into a cost-effective equipment for radiobiological studies: a proof of concept. *Sci Rep*. 2017;7(1):1-10. https://doi.org/10.1038/s41598-017-17543-3
7. Prezado Y, Jouvion G, Hardy D, et al. Proton minibeam radiation therapy spares normal rat brain: long-term clinical, radiological and histopathological analysis. *Sci Rep*. 2017;7(1):1-7. https://doi.org/10.1038/s41598-017-14786-y
8. Lamirault C, Doyère V, Juchaux M, et al. Short and long-term evaluation of the impact of proton minibeam radiation therapy on motor, emotional and cognitive functions. *Sci Rep*. 2020;10(1):13511. https://doi.org/10.1038/s41598-020-70371-w
9. Prezado Y, Jouvion G, Patriarca A, et al. Proton minibeam radiation therapy widens the therapeutic index for high-grade gliomas. *Sci Rep*. 2018;8(1):1-10. https://doi.org/10.1038/s41598-018-34796-8
10. Prezado Y, Jouvion G, Guardiola C, et al. Tumor control in RG2 glioma-bearing rats: a comparison between proton minibeam therapy and standard proton therapy. *Int J Radiat Oncol*. 2019;104(2):266-271. https://doi.org/10.1016/j.ijrobp.2019.01.080
11. Lamirault C, Brisebard E, Patriarca A, et al. Spatially modulated proton minibeams results in the same increase of lifespan as a uniform target dose coverage in F98-glioma-bearing rats. *Radiat Res*. 2020;194(6):715-723. https://doi.org/10.1667/RADE-19-00013.1
12. Sotiropoulos M, Brisebard E, Le Dudal M, et al. X-rays minibeam radiation therapy at a conventional irradiator: pilot evaluation in F98-glioma bearing rats and dose calculations in a human phantom. *Clin Transl Radiat Oncol*. 2021;27:44-49. https://doi.org/10.1016/j.ctro.2021.01.001
13. Prezado Y, Martínez-Rovira I, Thengumpallil S, Deman P. Dosimetry protocol for the preclinical trials in white-beam minibeam radiation therapy. *Med Phys*. 2011;38(9):5012-5020. https://doi.org/10.1118/1.3608908
14. Martínez-Rovira I, Sempau J, Prezado Y. Development and commissioning of a Monte Carlo photon beam model for the forthcoming clinical trials in microbeam radiation therapy. *Med Phys*. 2011;39(1):119-131. https://doi.org/10.1118/1.3665768
15. Peucelle C, Nauraye C, Patriarca A, et al. Proton minibeam radiation therapy: experimental dosimetry evaluation. *Med Phys*. 2015;42(12):7108-7113. https://doi.org/10.1118/1.4935868
16. Ocadiz A, Livingstone J, Donzelli M, et al. Film dosimetry studies for patient specific quality assurance in microbeam radiation therapy. *Phys Med*. 2019;65:227-237. https://doi.org/10.1016/j.ejmp.2019.09.071
17. Niroomand-Rad A, Chiu-Tsao ST, Grams MP, et al. Report of AAPM Task Group 235 radiochromic film dosimetry: an update to TG-55. *Med Phys*. 2020;47(12):5986-6025. https://doi.org/10.1002/mp.14497
18. Ciancaglioni I, Marinelli M, Milani E, et al. Dosimetric characterization of a synthetic single crystal diamond detector in clinical radiation therapy small photon beams. *Med Phys*. 2012;39(7 pt 1):4493-4501. https://doi.org/10.1118/1.4729739
19. Mandapaka A, Verona-Rinati G, Ghebremedhin A, Patyal B. Evaluation of the dosimetric properties of a synthetic single crystal diamond detector in clinical proton beams. *Med Phys*. 2013;40(12):227-227. https://doi.org/10.1118/1.4814539
20. Di Venanzio C, Marinelli M, Milani E, et al. Characterization of a synthetic single crystal diamond Schottky diode for radiotherapy electron beam dosimetry. *Med Phys*. 2013;40(2):021712. https://doi.org/10.1118/1.4774360
21. Papaconstadopoulos P, Tessier F, Seuntjens J. On the correction, perturbation and modification of small field detectors in relative dosimetry. *Phys Med Biol*. 2014;59(19):5937-5952. https://doi.org/10.1088/0031-9155/59/19/5937
22. Underwood TSA, Rowland BC, Ferrand R, Vieillevigne L. Application of the Exradin W1 scintillator to determine Ediode 60017 and microDiamond 60019 correction factors for relative dosimetry within small MV and FFF fields. *Phys Med Biol*. 2015;60(17):6669-6683. https://doi.org/10.1088/0031-9155/60/17/6669
23. Brace OJ, Alhujaili SF, Paino JR, et al. Evaluation of the PTW microDiamond in edge-on orientation for dosimetry in small fields. *J Appl Clin Med Phys*. 2020;21(8):278-288. https://doi.org/10.1002/acm2.12906
24. Livingstone J, Stevenson AW, Butler DJ, Häusermann D, Adam JF. Characterization of a synthetic single crystal diamond detector for dosimetry in spatially fractionated synchrotron x-ray fields. *Med Phys*. 2016;43(7):4283-4293. https://doi.org/10.1118/1.4953833
25. Hugtenburg RP, Reynard DDH. Monte Carlo based corrections for the dosimetry of x-ray microbeams with diamond detectors. *J Phys Conf Ser*. 2020;1662(1):012013. https://doi.org/10.1088/1742-6596/1662/1/012013
26. IAEA. Technical Reports Series No. 398: Absorbed Dose Determination in External Beam Radiotherapy. 2000. https://doi.org/10.1097/00004032-200111000-00017
27. Almond PR, Biggs PJ, Coursey BM, et al. AAPM's TG-51 protocol for clinical reference dosimetry of high-energy photon and electron beams. *Med Phys*. 1999;26(9):1847-1870. https://doi.org/10.1118/1.598691
28. Sempau J, Andreo P, Aldana J, Mazurier J, Salvat F. Electron beam quality correction factors for plane-parallel ionization chambers: Monte Carlo calculations using the Penelope system. *Phys Med Biol*. 2004;49(18):4427-4444. https://doi.org/10.1088/0031-9155/49/18/016

29. Perl J, Shin J, Schümann J, Faddegon B, Paganetti H. TOPAS: an innovative proton Monte Carlo platform for research and clinical applications. *Med Phys*. 2012;39(11):6818-6837. https://doi.org/10.1118/1.4758060
30. Faddegon B, Ramos-Méndez J, Schuemann J, et al. The TOPAS tool for particle simulation, a Monte Carlo simulation tool for physics, biology and clinical research. *Phys Med*. 2020;72:114-121. https://doi.org/10.1016/j.ejmp.2020.03.019
31. Bujila R, Omar A, Poludniowski G. A validation of SpekPy: a software toolkit for modelling X-ray tube spectra. *Phys Med*. 2020;75:44-54. https://doi.org/10.1016/j.ejmp.2020.04.026
32. Poludniowski G, Omar A, Bujila R, Andreo P. Technical note: SpekPy v2.0—a software toolkit for modeling x-ray tube spectra. *Med Phys*. 2021;48(7):3630-3637. https://doi.org/10.1002/mp.14945
33. De Marzi L, Patriarca A, Nauraye C, et al. Implementation of planar proton minibeam radiation therapy using a pencil beam scanning system: a proof of concept study. *Med Phys*. 2018;45(11):5305-5316. https://doi.org/10.1002/mp.13209
34. De Marzi L, Da Fonseca A, Moignier C, et al. Experimental characterisation of a proton kernel model for pencil beam scanning techniques. *Phys Med*. 2019;64:195-203. https://doi.org/10.1016/j.ejmp.2019.07.013
35. Schneider T, Patriarca A, Prezado Y. Improving the dose distributions in minibeam radiation therapy: helium ions vs protons. *Med Phys*. 2019;46:3640-3648. https://doi.org/10.1002/mp.13646
36. Rivera JN, Kierski TM, Kasoji SK, Abrantes AS, Dayton PA, Chang SX. Conventional dose rate spatially-fractionated radiation therapy (SFRT) treatment response and its association with dosimetric parameters—a preclinical study in a Fischer 344 rat model. *PLoS One*. 2020;15(6):e0229053. https://doi.org/10.1371/journal.pone.0229053

SUPPORTING INFORMATION

Additional supporting information can be found online in the Supporting Information section at the end of this article.

How to cite this article: Sotiropoulos M, Prezado Y. Radiation quality correction factors for improved dosimetry in preclinical minibeam radiotherapy. *Med Phys*. 2022;49:6716–6727. https://doi.org/10.1002/mp.15838